Diffraction of Light by Arrays of Colloidal Spheres

Irvin M. Krieger and Francis M. O'Neill

Contribution from the Department of Chemistry and Division of Polymer Science, Case Western Reserve University, Cleveland, Ohio. *Received November 30, 1967*

Abstract: Ordered arrays of colloidal spheres, which are found in monodisperse latexes at high concentration and in their dried noncoalesced monolayer films, exhibit with visible light many of the diffraction phenomena shown with X-rays by molecular crystals. Analogs of powder patterns and single-crystal patterns were studied experimentally, and the findings were compared with diffraction theory for two-dimensional crystalline arrays. Iridescence of monodisperse latexes is attributed to Bragg reflections from successive planes parallel to the sample surface. Diffraction from monodisperse latex arrays yields convenient and accurate particle size determination and also provides a simple experimental demonstration of diffraction theory in operation.

A latex is a surfactant-stabilized colloidal dispersion of spherical polymer particles in an aqueous medium. As formed by emulsion polymerization, a typical synthetic latex is polydisperse (has a broad particle size distribution) and appears milk-white in color. Special polymerization techniques have recently been developed which yield monodisperse latexes, *i.e.*, of highly uniform particle size. When the particle diameter falls in the range 0.15–0.50 μ and the volume fraction of polymer exceeds 35%, these latexes frequently display a striking iridescence, similar to that of precious opals. A different color phenomenon is shown by thin noncoalesced films laid down on transparent substrates by drying monodisperse latexes of diameters greater than 0.4 μ. In view of the unpigmented nature of the particles, the requirement of high uniformity of particle size, and the frequent occurrence of crystal-like formations in the concentrated latexes, it is evident that these color phenomena are due to diffraction by arrays of particles. A third color phenomenon, observed in highly dilute latexes and attributable to Mie scattering by individual latex spheres, was not investigated in this study.

The first monodisperse latexes were of polystyrene and were produced by the Dow Chemical Co. in 1947; in 1954 Alfrey, Bradford, Vanderhoff, and Oster[1] published the first major study of their optical properties. These authors attributed the reflection from thick dried films to scattering by hexagonal two-dimensional arrays of spheres, but their data agreed with theory only in the limit of zero angle between the incident beam and the sample surface. Scattering by transparent films of particles was attributed to Fraunhofer diffraction from independent spherical scatterers. Noting that Mie's theory[2] should apply, they chose instead to employ a simple empirical relationship which correlated their data.

Subsequently, Luck, Wesslau, and Klier[3,4] studied reflection and transmission of visible light by concentrated polyacrylate latexes, and successfully interpreted their observations in terms of Bragg diffraction from three-dimensional arrays. They also showed that monolayers of particles illuminated under normal incidence by monochromatic light gave diffraction patterns similar in appearance to Debye–Scherrer X-ray powder patterns.

In recent years, this laboratory has prepared monodisperse latex samples of sizes ranging from 0.07 to 1.3 μ at high volume fractions. In an attempt to understand quantitatively the origin of the iridescence shown by many samples, optical studies similar to those of previous investigators were initiated. It soon became apparent that the higher uniformity and increased range of particle sizes now at hand, together with improved experimental methods, permitted a more definitive study than was previously feasible.

Experimental Study of Scattering by Thin Films

References 1, 3, and 4 show typical micrographs of monodisperse latexes. One would expect that such highly ordered monolayers of uniform spheres would give rise to diffraction of electromagnetic radiation whose wavelength is comparable to the array spacing. An extensive monolayer sample can readily be prepared by drying a smear of diluted latex on a glass microscope slide. Viewed by transmitted white light, such a sample acts as an inefficient color filter; spectrophotometric measurement of absorption *vs.* wavelength reveals broad absorption bands (Figure 1). When a slide is mounted on the table of a light-scattering photometer as in Figure 2 and illuminated by monochromatic light, the graph of scattered intensity *vs.* angle (Figure 3) shows distinct peaks.

In order to test whether this phenomenon is due to order in two or in three dimensions, a silicon monoxide replica of the film was prepared and mounted in the photometer. As may be seen from Table I, the replica gave peaks at the same angles as the original, proving (1) that the effect arises from a two-dimensional array, and (2) that it is the array geometry rather than the

Table I. Comparison of Scattering Maxima for Latex Film and Replica[a]

Wavelength, Å	θ_2(latex), deg	θ_2(replica), deg
4360	1.5	1.6
4360	47.3	47.5
5460	75.2	75.0

[a] 0.585-μ poly(vinyltoluene) latex and SiO replica; $\theta_1 = 60°$.

(1) T. Alfrey, Jr., E. B. Bradford, J. W. Vanderhoff, and G. Oster, *J. Opt. Soc. Am.*, **44**, 603 (1954).
(2) G. Mie, *Ann. Physik*, **25**, 377 (1908).
(3) W. Luck, M. Klier, and H. Wesslau, *Ber. Bunsenges. Phys. Chem.*, **67**, 75, 84 (1963); *Naturwissenschaften*, **50**, 485 (1963).
(4) W. Luck and H. Wesslau, "Festschrift Carl Wurster," Gesamtherstellung Johannes Weisbecker, Frankfurt-am-Main, 1960.

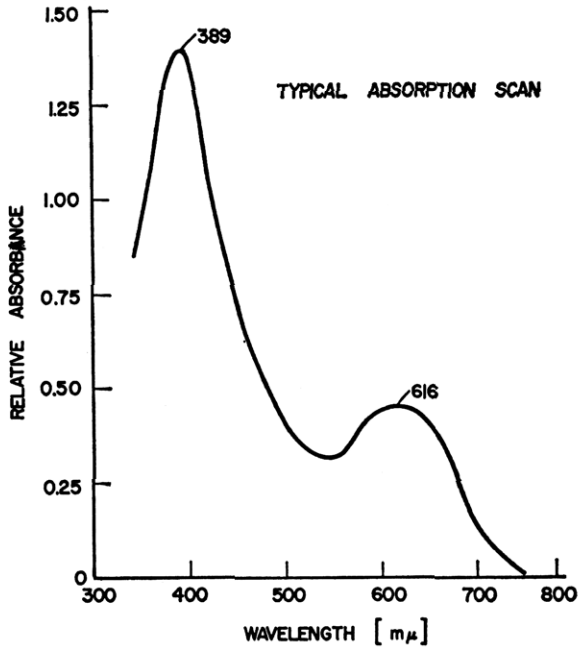

Figure 1. Absorption spectrum of dried film of 0.26-μ polystyrene latex.

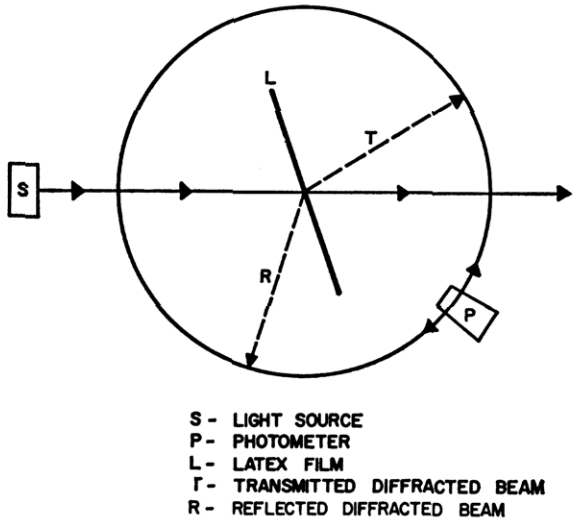

Figure 2. Schematic representation of scattering photometer modified to align monolayer films at various inclinations to the incident beam.

shape and composition of the scatterers that determines the locations of the peaks.

When a monolayer sample is illuminated by an intense normally incident monochromatic beam, a pattern of concentric rings is observed on a screen behind the film (Figure 4). When the sample is tilted with respect to the primary beam, the pattern of Figure 5 is observed; the arrow on the figure shows the direction of travel of the photocell in photometric experiments such as that of Figure 10.

From the strong resemblance to Debye–Scherrer–Hull patterns[5] for the scattering of X-rays by polycrystalline solids and to Thomson's electron diffraction patterns from metal foils,[6] it seemed probable that the

(5) P. Debye and R. Scherrer, *Physik. Z.*, **17**, 277 (1916); **18**, 291 (1917).
(6) G. P. Thomson, *Proc. Roy. Soc.*, (London), **117**, 600 (1928).

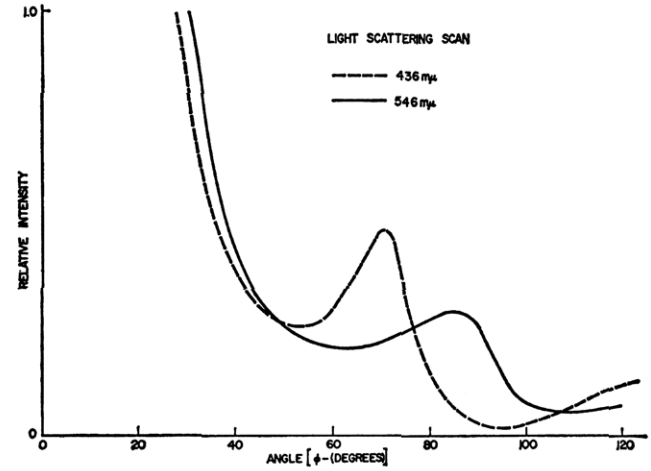

Figure 3. Scattering photometer scan at two wavelengths of dried monolayer of 0.405-μ polystyrene latex (normal incidence).

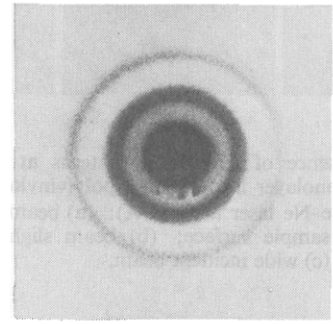

Figure 4. Optical diffraction pattern from monodisperse latex film: poly(vinyltoluene) latex of 3.0-μ diameter (He–Ne laser source of λ = 6328 Å at normal incidence).

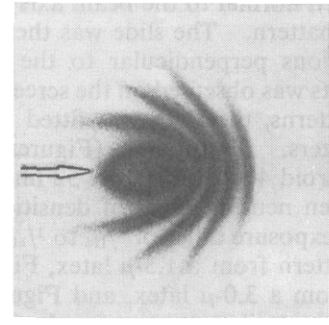

Figure 5. Optical diffraction pattern from inclined monodisperse latex film; same sample and light source as in Figure 4, but with θ = 45°.

scattering patterns for visible light from dried latex films (and their replicas) arises from diffraction by a "polycrystalline" array. This opinion gained further strength from the polycrystalline appearance of many of the micrographs.

A concerted program was initiated to obtain a diffraction pattern from a monocrystalline area. Early results of efforts to produce larger areas of monocrystalline perfection were discouraging. The alternative approach, that of narrowing the incident beam so that it impinged on a two-dimensional single crystal, met with success, however. A low-power helium–neon laser beam (Optics Technology Inc., Model 170; output 0.3 mW at 6238 Å) was focused with a converging

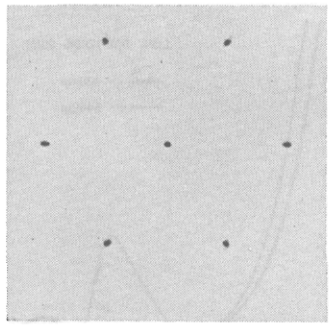

Figure 6. Photograph of diffraction pattern from two-dimensional single crystal of 1.293-μ poly(vinyltoluene) latex particles: source, He–Ne laster at 6238 Å; sample-to-screen distance, 4.34 cm (one-half actual size).

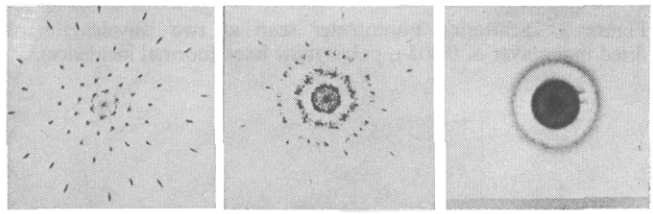

a b c

Figure 7. Sequence of diffraction patterns at increasing beam widths, from monolayer film of 3.0-μ poly(vinyltoluene) latex particles (source, He–Ne laser at 6238 Å): (a) beam focused to minimum width at sample surface; (b) beam slightly defocused at sample surface; (c) wide incident beam.

lens onto the surface of the slide, which was held in a microscope stage manipulator; a minimum beam diameter of 70 μ was found to be obtainable.

The apparatus was set up in a dark room, with a screen mounted normal to the beam axis to observe the transmission pattern. The slide was then manipulated in two directions perpendicular to the beam until a pattern of spots was observed on the screen. To photograph the patterns, the laser was fitted with a shutter and neutral filters. Photographs (Figures 6 and 7) were taken on Polaroid 4 × 5 Pola Pan 52 film packs, using Kodak Wratten neutral filters of densities 1.2 and 3.0 in series, and exposure times of $^1/_{125}$ to $^1/_{500}$ sec. Figure 6 shows a pattern from a 1.3-μ latex, Figure 7a shows the pattern from a 3.0-μ latex, and Figures 7b and 7c result from successive stages of enlargement of the beam size, showing exactly how the spots on the single-crystal pattern become rings on the polycrystalline "powder pattern."

Theory of Scattering by a Two-Dimensional Array

When light is diffracted by a regular array of scatterers, the geometry of the scattering pattern is determined by the periodicity of the array, while the relative intensities of the spots or lines depend upon properties of the individual scatterers.[7] In mathematical terms, the scattered light intensity I is the product of a sharply peaked interference function $|F|^2$ of the array and a slowly varying intensity function G of the individual scatterer.

$$I = G|F|^2 \tag{1}$$

(7) M. Born and E. Wolf, "Principles of Optics," 2nd ed, The Macmillan Co., New York, N. Y., 1964.

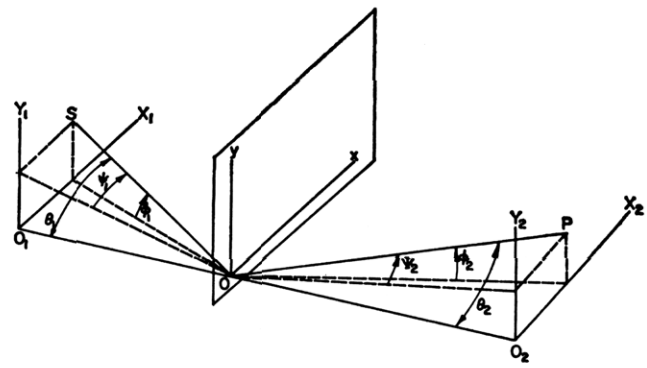

Figure 8. System of coordinates for discussion of theory of diffraction by two-dimensional array of scatterers.

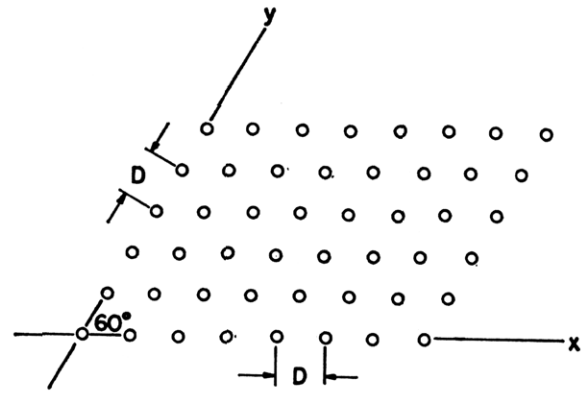

Figure 9. Geometry of hexagonal two-dimensional scattering array. Here $\alpha = 60°$.

Since the interpretations which follow will be based on the positions of the diffraction maxima rather than their intensities, only the theory of the interference function need be considered here.

Figure 8 shows the coordinate system of the diffraction experiments. The (x, y) plane contains the sample, the (x_1, y_1) plane the source S, located by angles θ_1, ϕ_1, ψ_1, and the (x_2, y_2) plane the detector P, defined by θ_2, ψ_2, ϕ_2. Both sets of angles obey the relation

$$\sin^2 \psi + \sin^2 \phi = \sin^2 \theta \tag{2}$$

The sample array of Figure 9 is rhomboidal and is characterized by a spacing D and an angle α. The scattering sources are thus located at points (x_{jr}, y_{jr}) such that j and r are integers and

$$x_{jr} = (j - 1)D + (r - 1)D \sin \alpha \tag{3}$$

$$y_{jr} = (r - 1)D \cos \alpha \tag{4}$$

For this geometry the function F is given by

$$F = \sum_{j=1}^{N} \sum_{r=1}^{M} \exp\{ik[x_{jr}(\sin \psi_1 + \sin \psi_2) + y_{jr}(\sin \phi_1 + \sin \phi_2)]\} \tag{5}$$

where $k = 2\pi/\lambda$. Combining eq 3–5, together with the identity

$$\sum_{r=0}^{R+1} a^r = (1 - a)^{-1}(1 - a^R) \tag{6}$$

it can be shown that

$$|F^2| = \frac{\sin^2 N\pi\xi}{\sin^2 \pi\xi} \frac{\sin^2 M\pi\eta}{\sin^2 \pi\eta} \quad (7)$$

with

$$\xi = \lambda^{-1}D(\sin \psi_1 + \sin \psi_2) \quad (8)$$

$$\eta = \lambda^{-1}D \sin \alpha (\sin \psi_1 + \sin \psi_2) + \cos \alpha (\sin \phi_1 + \sin \phi_2) \quad (9)$$

Diffraction maxima thus occur for integral values m_1 and m_2 of ξ and η, respectively. For the particular case of a hexagonal array under normal incidence, $\alpha = \pi/3$, $\psi_1 = 0$, $\phi_1 = 0$, and hence

$$m_1 = \lambda^{-1}D \sin \psi_2 \quad (10)$$

$$m_2 = \lambda^{-1}D[1/2 \sin \psi_2 + (\sqrt{3/2}) \sin \phi_2] \quad (11)$$

Solution for ψ_2 and ϕ_2, together with eq 2, yields

$$(m_1^2 - m_1m_2 + m_2^2)^{1/2}\lambda = (\sqrt{3}/2)D \sin \theta_2 \quad (12)$$

For oblique incidence, with θ_1 and θ_2 measured in the same plane, the conditions for diffraction maxima are

$$(m_1^2 - m_1m_2 + m_2^2)\lambda = (\sqrt{3}/2)D(\sin \theta_1 + \sin \theta_2) \quad (13)$$

If we let $d = (\sqrt{3}/2)D$ be the spacing between rows of scatterers and also let $m = (m_1^2 - m_1m_2 + m_2^2)^{1/2}$, eq 13 becomes identical in form with the "grating equation" which, with m integral, defines the positions of scattering maxima obtained when a ruled grating is substituted for the scattering array. Table II shows how various values of m arise, with the number of spots for each m value.

Table II. Parameters for Diffraction from Two-Dimensional Hexagonal Array

Indices ± (m_1,m_2)	m	Number of spots
(1,0)(0,1)(1,1)	1.00	6
(2,1)(1,2)(1,$\bar{1}$)	$\sqrt{3}$ = 1.73	6
(2,0)(0,2)(2,2)	2.00	6
(2,$\bar{1}$)($\bar{1}$,2)(3,1)(3,2)(2,3)	$\sqrt{7}$ = 2.65	12
(3,0)(0,3)(3,3)	3.00	6
(4,2)(2,4)(2,$\bar{2}$)	$\sqrt{12}$ = 3.46	6
($\bar{1}$,3)(3,$\bar{1}$)(1,4)(4,1)(4,3)(3,4)	$\sqrt{13}$ = 3.61	12
(4,0)(0,4)(4,4)	4.00	6
(2,$\bar{3}$)($\bar{3}$,2)(2,5)(5,2)(3,5)(5,3)	$\sqrt{19}$ = 4.36	12
(1,$\bar{4}$)($\bar{4}$,1)(1,5)(5,1)(4,5)(5,4)	$\sqrt{21}$ = 4.58	12
(5,0)(0,5)(5,5)	5.00	6

Comparison of Theory with Experiment

A series of 12 monodisperse polystyrene and poly(vinyltoluene) latexes was used in this study, ranging in diameter from 0.18 to 3 μ. The two largest samples were obtained from the Dow Chemical Co.; all others were prepared by emulsion polymerization in this laboratory. Samples for electron-photomicrographic determination of particle diameter were prepared by a standard technique;[8] micrographs of the sample and of a standard ruled grating were taken at the same magnification. Optical micrographs were taken of the larger samples (and of a calibration grating), and a method similar to that of Kubitschek[9] was employed to obtain the packing diameter, by measuring the length of a linear array containing a known number of particles. Table III shows the diameters obtained for the samples reported here. A uniformity index U, defined as the ratio of the weight-average particle diameter to the number average, was determined from the electron micrographs for each sample. For all except sample A, the uniformity index was less than 1.01; sample A was bimodal, with *ca.* 90% of the particles having the indicated diameter of 3.075 μ and *ca.* 10% having diameters of 4.0 μ.

Table III. Measurements of Particle Diameters by Microscopy

Sample	Diameter, μ (electron microscopy)	Packing diameter, μ (optical microscopy)
A	3.075	3.00
B	1.925	1.910
C	1.293	1.285
D	0.905	0.885
E	0.635	
F	0.440	
G	0.1825	
H	0.1885	
I	0.1930	
J	0.2180	
K	0.2295	
L	0.2542	

Techniques employed to prepare film samples included (1) painting a smear of concentrated latex on a glass or Mylar (polyethylene terephthalate) substrate, and (2) pressing a drop of latex between two flat glass surfaces which were then separated; both techniques were found to produce large monolayer areas with hexagonal packing in the dried films. The sample-cell table of a Brice–Phoenix light-scattering photometer was adapted to incline the film slides at various angles to the primary beam as shown in Figure 2. A ten-turn helical potentiometer was coupled to the photometer turn-table by a rubber disk; when connected to a small battery the potentiometer gave a voltage signal which varied lineally with the angular position of the photodetector. Graphs such as that of Figure 10 for oblique incidence and Figure 11 for normal incidence were obtained on an X–Y recorder with the potentiometer signal on the X axis and the phototube output on the Y axis, with slow manual rotation of the turn-table.

Table IV shows values of $m = (m_1^2 - m_1m_2 + m_2^2)^{1/2}$ calculated from the intensity peaks of Figure 10, using eq 13 with D = 3.075 μ. The comparison with theoretical m values is quite good, except for the first two peaks. It is noteworthy that the use of a D value of 3.00 μ, obtained by the Kubitschek method from

Table IV. Experimental (italicized) and Theoretical m Values for Data of Figure 13

0.86, 1.00 *1.66*, 1.73, 2.00, *2.64*, 2.65, 3.00, 3.46, *3.53*, 3.61, 4.00, 4.36, *4.45*, 4.58, 5.00, 5.19, 5.30, *5.35*, 6.00, *6.23*, 6.92, 7.00, *7.12*, 8.00, *8.09*

(8) S. H. Maron, C. Moore, and A. S. Powell, *J. Appl. Phys.*, **23**, 900 (1952).

(9) H. E. Kubitschek, *Nature*, **192**, 1188 (1961).

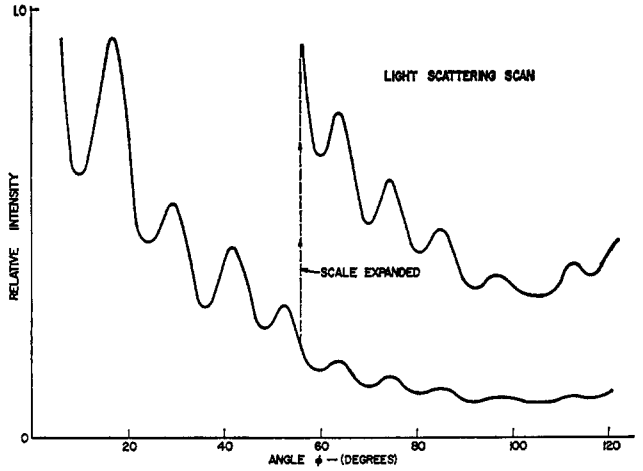

Figure 10. Photometer scan from monolayer film of 3.0-μ poly(vinyltoluene) latex particles inclined at $\theta_1 = 60°$ (source, Hg vapor lamp with filter to give monochromatic light at 5460 Å).

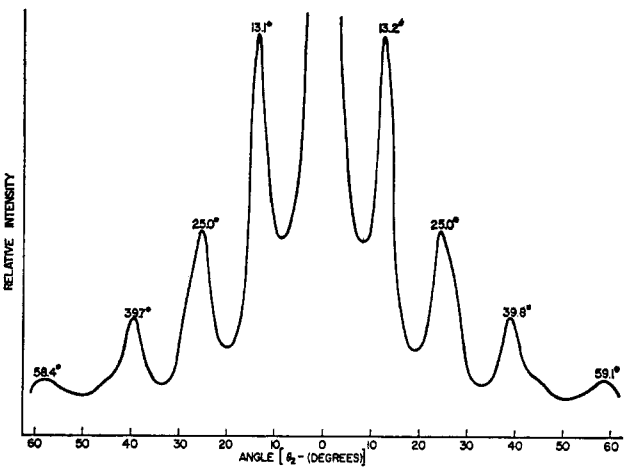

Figure 11. Photometer scan from same monolayer film as in Figure 10, but at normal incidence (source, He–Ne laser at 6238 Å).

optical micrographs, would have improved the agreement for the higher order peaks. Note also that several of the theoretical peaks are absent, due presumably to the influence of the intensity function G of eq 1. Table V shows diameters for sample A calculated for each of the peaks of Figure 10, including shoulders at 27.5 and 45.0° (which are more evident on the original scan than on the figure). Again the two innermost peaks give the least accurate results. Table VI shows a similar analysis of reflection data for sample C obtained at two different wavelengths and two different sample inclinations. Finally, Table VII summarizes the results of measurements on samples A–F by this technique; the smaller samples did not give peaks at suitably low angles for measurement.

Table V. Diameters for Sample A Computed from Data of Figure 14

θ_2, deg[a]	Assumed m	D, μ
13.2	1.00	3.20
25.0	1.73	2.99
27.5*	2.00	3.16
39.8	2.65	3.03
45.0*	3.00	3.10
58.8	3.46	2.96

[a] Asterisk indicates shoulder; other values represent peaks.

Table VI. Diameters for Sample C from Reflection Data

λ, Å	θ_1, deg	θ_2, deg	m	D, μ
4360	60	−30.1	1.00	1.38
		−5.3	2.00	1.30
		+10.5	2.65	1.27
5460	60	−23.6	1.00	1.30
		−1.5	1.73	1.30
		+6.5	2.00	1.29
4360	75	−37.0	1.00	1.38
		−16.8	1.73	1.29
		−11.2	2.00	1.31
		+3.9	2.65	1.29
		+11.8	3.00	1.29
		+26.3	3.61	1.29
5460	75	−29.8	1.00	1.35
		−7.4	1.73	1.30
		+0.1	2.00	1.30
		+18.6	2.65	1.30

Table VII. Summary of Diameters for Six Samples from Photometer Scans

Sample	λ, Å	No. of peaks	D, μ
A	4360	9	3.140
	5460	9	3.148
	6328	11	3.003
B	4360	7	1.986
	5460	6	1.975
	6328	6	1.944
C	4360	4	1.370
	5460	3	1.375
	6328	3	1.332
D	4360	4	0.881
	5460	3	0.887
	6328	2	0.924
E	4360	2	0.654
	5460	1	0.688
F	4360	1	0.469

Defining measurements for the single-crystal diffraction experiments were made in order to permit determination of the scattering angles θ_2 of the observed spots. Table VIII summarizes the diameters obtained from eq 13 and these data. The agreement here provides excellent confirmation of the accuracy of the

Table VIII. Summary of Diameters from Single-Crystal Patterns

Sample	θ_2, deg	m	D, μ
A	14.0	1.00	3.028
	24.8	1.73	3.028
	28.5	2.00	3.045
	39.5	2.65	3.035
	46.1	3.00	3.038
	56.3	3.46	3.030
	59.8	3.61	3.055
B	22.1	1.00	1.940
	40.6	1.73	1.940
	49.0	2.00	1.885
C	33.8	1.00	1.315

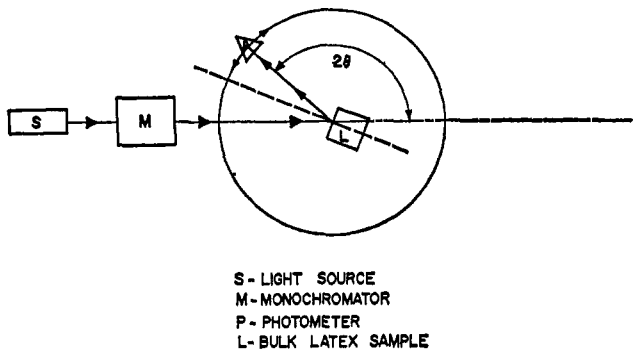

Figure 12. Schematic representation of optical diffractometer used for measuring reflectance spectra of concentrated monodisperse latexes. Angles of incidence and reflection were equal.

method and of the applicability of the theory of diffraction from a two-dimensional hexagonal array.

Scattering by Concentrated Monodisperse Latexes.

The iridescence displayed by concentrated monodisperse latexes of particle diameters in the 0.17–0.55-μ range was attributed by Luck, *et al.*, to Bragg reflections from successive planes of close-packed spheres aligned parallel to the surface so as to present the 111 planes of a face-centered cubic array. If D_p is the packing diameter of the spheres, then spacing between planes is $D_p \sqrt{3}/2$, whether the lattice is face-centered cubic or hexagonal close packed. The correct wavelength to use in the Bragg relation is the wavelength in the medium $\lambda_m = \mu\lambda_0$, where μ is the refractive index of the medium and λ_0 the *in vacuo* wavelength of the incident radiation. Thus Bragg's law gives

$$n\mu\lambda_0 = \sqrt{3}D_p \sin\theta \qquad (14)$$

To test the validity of eq 14, a photometer was set up according to the diagram of Figure 12. The source was a tungsten lamp, the monochromator a Bausch and Lomb Model 33-86-02, and the sample holder a glass cell with an optically flat side. With the photodetector positioned so that the angle of incidence equalled the angle of reflection, the reflection spectrum of Figure 13 was measured. At the frequency corresponding to the reflectance maximum, extinction of scattered light was observed at all other angles. The extinction, which was visually observed as a darkening of the sample surface, was sufficiently sharp to permit accurate location of the reflectance peak.

Table IX. Summary of Packing Diameters from Reflectance Spectra of Latexes

Sample	2θ, deg	λ_0 at peak, Å	D_p, μ
G	141.7	4220	1.845
(1.825 μ)	158.0	4270	1.795
H	143.0	4350	1.890
(1.885 μ)	158.0	4390	1.845
I	138.4	4380	1.930
(1.930 μ)	157.6	4480	1.885
J	140.0	4850	2.130
(2.180 μ)	156.4	4920	2.070
K	140.0	5200	2.285
(2.295 μ)	157.1	5260	2.215
L	139.2	6060	2.670
(2.542 μ)	157.2	6170	2.590

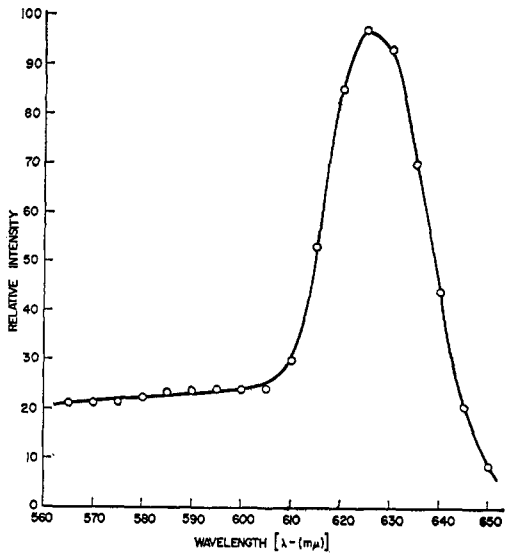

Figure 13. Typical reflectance spectrum of a concentrated monodisperse latex. Sample: 0.261-μ polystyrene latex at 45% polymer content; $\theta = 81°$.

Using the peak reflectance wavelengths in eq 14, together with a value of 1.40 for μ, values of D_p were determined for samples G–L. Table IX compares the values of D_p with the diameter values D measured by electron microscopy. Within the error of measurement, therefore, the packing diameter may be taken as the particle diameter.

Visual observation of the iridescence of a sample illuminated by white light frequently shows two colors, *e.g.*, purple and yellow for 0.18-μ latex, blue and pink for 0.22-μ latex. This dichroism may be interpreted as spectral reflection at the Bragg wavelength for the angle of observation (usually $\theta \sim 90°$), plus diffuse scattering of the color complement at other angles.

Conclusions

The experiments reported here show conclusively that, contrary to the assumptions of Alfrey, *et al.*, the scattering by monolayer films of monodisperse latex is due to the two-dimensional periodicity of the array. "Powder patterns" or the equivalent photometer scans of polycrystalline arrays can be used to determine particle sizes above 0.4 μ. Diameters calculated from the two innermost peaks or rings are less accurate than those obtained from the third peak and those of higher order.

Single-crystal patterns can be obtained from noncoalesced films formed from latexes of particle diameters in the micron range. This observation has also been made by K. A. Jackson and collaborators at the Bell Telephone Laboratories (private communication). Diameters calculated from single-crystal measurements are highly accurate and reproducible. The apparatus and techniques for obtaining both single-crystal and polycrystalline diffraction patterns are simple enough to serve as lecture-demonstration or student laboratory experiments to illustrate qualitative and quantitative aspects of diffraction theory.

Iridescence of concentrated monodisperse latexes is due to Bragg reflections from successive planes of spheres packed parallel to the sample surface. Measurement of the layer spacing using Bragg techniques

furnishes a convenient and accurate determination of particle diameter.

None of the methods of study employed here has been applied to all of the available samples. The limitations are imposed by the availability of sources and, in some cases, by the geometries of the measuring apparatus. With light sources in the near-ultraviolet, the powder pattern technique could be extended to smaller samples. A blue laser would facilitate single-crystal studies, while sources and detectors in the near-infrared would permit the latex reflectance studies to be applied to the larger particle diameters.

Acknowledgments. The research described in this paper was supported in part by a Public Health Service grant. Funds from a Paint Research Institute fellowship grant were used to purchase the optical equipment employed in the single-crystal studies.

The Electrical Conductivity of Some Acridizinium Compounds

John Bashaw[1] and Paul M. Gross[2]

Contribution from the Department of Chemistry, Duke University, Durham, North Carolina. *Received December 1, 1967*

Abstract: Measurements of the electrical conductivity (dark) of the following solid acridizinium-type compounds have been made over a range of temperatures and the activation energies for conduction determined. These included acridizinium bromide, perchlorate, and anthraquinone-2-sulfonate and the betaine of 9-sulfoacridizinium hydroxide (a zwitterion), as well as the conductivity of a higher member of the series, 12a,14a-bis(azonia)pentaphene.

In recent years fairly extensive measurements have been made of the electrical conductivity of solid organic compounds of certain classes such as polynuclear hydrocarbons, long-chain polymers, and dyes.[3] Since no electrical measurements have been reported on compounds of the general type of acridizinium bromide (I), the dark conductivity of I was determined as well as

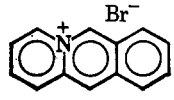

I

that of a series of related compounds. These included two other salts, acridizinium perchlorate (II) and anthraquinone-2-sulfonate (III), the betaine of 9-sulfoacridizinium hydroxide (IV), which is a zwitterion, and

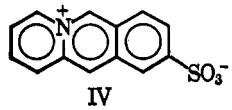

IV

the hydrate (V) and dimer (VI) of acridizinium bromide. Measurements were also made on a higher member of the series, 12a,14a-bis(azania)pentaphene dibromide (VII).

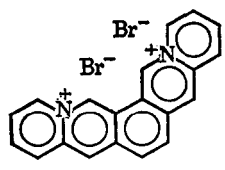

VII

The acridizinium cation in some of these compounds has a fairly close structural similarity to the anthracene molecule, and the conjugated ring system involved is essentially the same as that found in a number of other organic semiconductors. In view of this, a number of measurements on anthracene were carried out to provide a reliable comparison base for the data, using the same apparatus and procedural techniques as those employed for the acridizinium compounds.

The series of salts (I–III) was of interest in connection with possible ionic contributions to the conductivity because of the wide variance in the size of the anions involved, and the conductivity data for the zwitterion IV provided a comparison case in which such ionic contributions were not possible. The fact that the bromide (I) is actually prepared first as a monohydrate (V) made it possible to determine and compare the conductivity of the hydrated and anhydrous forms, a matte orf considerable interest as there are very little data in the literature regarding the conductivity of hydrates.

Experimental Section

A. Materials. Acridizinium bromide (I) was prepared by the method of Parham.[4] The cyclic acetal of picolinaldehyde [2-(1,3-dioxolan-2-yl)pyridine] was mixed with 10% excess of benzyl bromide and dissolved in the minimum possible amount of tetramethylene sulfone; the mixture kept 2 days at room temperature. The viscous product was washed (ethyl acetate), dissolved (methanol), and crystallized (methanol–ethyl acetate), and the resulting white quaternary salt was cyclized by refluxing for 18 hr in 50% HBr. The HBr was removed *in vacuo* giving crude yellow acridizinium bromide (85% yield) which was crystallized alternately from ethyl acetate–methanol, and from H_2O until a constant melting point was obtained. The final product melted with decomposition at 245–246° and was a monohydrate which on prolonged drying at 110° lost 6.5% of its weight (calculated loss, 6.48%) to give the anhydrous acridizinium bromide.

(1) Based in part on the dissertation submitted by J. D. Bashaw for the degree of Doctor of Philosophy at Duke University.

(2) Author to whom inquiries should be addressed.

(3) F. Guttman and L. E. Lyons, "Organic Semiconductors," John Wiley and Sons, Inc., New York, N. Y., 1967, *cf.* pp 706–767.

(4) J. C. Parham, Ph.D. Thesis, Duke University, Durham, N. C., 1963.